Inhibition of excessive mitophagy by N-acetyl-L-tryptophan confers hepatoprotection against Ischemia-Reperfusion Injury in rats

Huiting Li [Equal first author, 1] , **Yitong Pan** [Equal first author, 1] , **Hongjuan Wu** [2] , **Shuna Yu** [1] , **Jianxin Wang** [1] , **Jie Zheng** [3] , **Can Wang** [1] , **Jianguo Li** [Corresp., 1] , **Jiying Jiang** [Corresp. 1]

[1] Department of Anatomy, Weifang Medical University, Weifang, China

[2] Morphology Lab, Weifang Medical University, Weifang, China

[3] Department of Pathology, Weifang Medical University, Weifang, China

Corresponding Authors: Jianguo Li, Jiying Jiang
Email address: ljg7111@wfmc.edu.cn, jiangjy@wfmc.edu.cn

In order to investigate the mechnism of hepatoprotective of N-acetyl-L-tryptophan (L-NAT) against ischemia-reperfusion (I/R) injury, the effects of L-NAT were investigated in hepatic ischemia-reperfusion injury (HIRI) models both in vitro and in vivo, which were made by BRL cells and Sprague-Dawley (SD) rats, respectively. The cell viability of hepatocyte was assessed by cell counting kit-8 (CCK-8) staining. The activation of autophagy was detected by electron microscopy (EM), quantitative real-time PCR (qRT-PCR), Western Blotting and immunofluorescence. The activation of mitophagy was determined by the change of autophagy related protein, change of mitochondrial structure and function, co-location of autophagy protein and MitoTracker. Results showed that the morphological structures of hepatocytes were changed significantly after HIRI, and the cell viability of hydrogen peroxide (H_2O_2)-induced BRL cells was decreased. Autophagy markers Beclin1, microtubule associated protein 1 light chain 3-Ⅱ (LC3-Ⅱ) and autophagy related protein-7 (ATG-7) were highly expressed and the expression of SQSTM1 (P62) was decreased after HIRI, which suggested that autophagy of hepatocytes was activated after I/R. The reduction of ATP, mitochondrial DNA (mtDNA) and the mitochondrial transmembrane potential (ΔΨm) after H_2O_2-induced revealed that function of mitochondrial had also undergone significant changes. The increased expression of autophagy protein, destructure of mitochondria and mitochondrial dysfunction, the increased co-location of Beclin1 and MitoTracker induced by H_2O_2 implied the excessive mitophagy. The expression of autophagy protein was increased by 3-Methyladenine (3-MA), providing another piece of evidence. Importantly, all changes were restored by L-NAT pretreament. In conclusion, the present findings demonstrate that excessive mitophagy involved in the process of HIRI and L-NAT may protect hepatocytes against HIRI by inhibiting activation of mitophagy and improving the structure and function

of mitochondria.

1 **Inhibition of excessive mitophagy by N-acetyl-L-tryptophan confers**

2 **hepatoprotection against Ischemia-Reperfusion Injury in rats**

3 Huiting Li[1,*], Yitong Pan[1,*], Hongjuan Wu[2], Shuna Yu[1], Jianxin Wang[1], Jie Zheng[3], Can Wang[1],

4 Jianguo Li[1,#], Jiying Jiang[1,#]

5 *[1]Department of Anatomy, Weifang Medical University, Weifang, Shandong Porvince 261053,*

6 *China*

7 *[2]Morphology Lab, Weifang Medical University, Weifang, Shandong Porvince 261053, China*

8 *[3]Department of Pathology, Weifang Medical University, Weifang, Shandong Porvince 261053,*

9 *China*

10 *These authors contributed equally to this work.

11 Corresponding Author:

12 Jianguo Li

13 West Baotong Street. Weifang, Shandong Porvince 261053, China

14 Email address: ljg7111@wfmc.edu.cn

15 Jiying Jiang

16 West Baotong Street. Weifang, Shandong Porvince 261053, China

17 Email address: jiangjy@wfmc.edu.cn

18 **Abstract**

19   In order to investigate the mechnism of hepatoprotective of N-acetyl-l-tryptophan (L-NAT)

20 against ischemia-reperfusion (I/R) injury, the effects of L-NAT were investigated in hepatic

21 ischemia-reperfusion injury (HIRI) models both in vitro and in vivo, which were made by BRL

22 cells and Sprague-Dawley (SD) rats, respectively. The cell viability of hepatocyte was assessed

23 by cell counting kit-8 (CCK-8) staining. The activation of autophagy was detected by electron

24 microscopy (EM), quantitative real-time PCR (qRT-PCR), Western Blotting and

25   immunofluorescence. The activation of mitophagy was determined by the change of autophagy

26   related protein, change of mitochondrial structure and function, co-location of autophagy protein

27   and MitoTracker. Results showed that the morphological structures of hepatocytes were changed

28   significantly after HIRI, and the cell viability of hydrogen peroxide (H_2O_2)-induced BRL cells

29   was decreased. Autophagy markers Beclin1, microtubule associated protein 1 light chain 3-Ⅱ

30   (LC3-Ⅱ) and autophagy related protein-7 (ATG-7) were highly expressed and the expression of

31   SQSTM1 (P62) was decreased after HIRI, which suggested that autophagy of hepatocytes was

32   activated after I/R. The reduction of ATP, mitochondrial DNA (mtDNA) and the mitochondrial

33   transmembrane potential ($\Delta\Psi$m) after H_2O_2-induced revealed that function of mitochondrial had

34   also undergone significant changes. The increased expression of autophagy protein, destructure

35   of mitochondria and mitochondrial dysfunction, the increased co-location of Beclin1 and

36   MitoTracker induced by H_2O_2 implied the excessive mitophagy. The expression of autophagy

37   protein was increased by 3-Methyladenine (3-MA), providing another piece of evidence.

38   Importantly, all changes were restored by L-NAT pretreament. In conclusion, the present

39   findings demonstrated that excessive mitophagy involved in the process of HIRI and L-NAT

40   may protect hepatocytes against HIRI by inhibiting activation of mitophagy and improving the

41   structure and function of mitochondria.

42   **Keywords:** Hepatic ischemia-reperfusion injury; H_2O_2; N-acetyl-L-tryptophan; Mitophagy

43   **Introduction**

44   Hepatic ischemia-reperfusion injury (HIRI) occurs in many clinical situations, including

45   hepatic trauma, hypoperfusion due to vascular obstruction or hypovolemic shock, liver

46   transplantation, and liver tumors resection (*Selzner et al., 2003*). Ischemia-reperfusion (I/R)

47   injury during liver surgery and liver transplantation is regarded as the primary cause of liver

48   failure. HIRI is also a source of major complications in clinical practice affecting perioperative

49   morbidity, mortality, and recovery (*Park et al., 2009; Kalimeris et al., 2016*). Although many

50   different therapeutic interventions have been explored, there are still no effective treatments to

51   prevent HIRI. Therefore, it is necessary to explore effective therapeutic interventions in HIRI.

52   During the process of HIRI, the elevated reactive oxygen species (ROS) level and

53   subsequently depletion of endogenous antioxidants result in total breakdown of the endogenous

54   antioxidant defense and the failure of protecting the hepatocytes from oxidative damage (*Ji et al.,*

55   *2012; Lin et al., 2016; Shadel et al., 2015*). Numerous evidences indicate that mitochondria are

56   main source of ROS, and extremely susceptible to oxidative damage (*Singh et al., 2019*).

57   Moreover, ROS mediated mitochondrial oxidative damage compel to more production of ROS.

58   The elevated ROS can either directly or indirectly lead to mitochondrial dysfunction. Therefore,

59   removal of damaged mitochondria by mitophagy is essential for the physiological function of

60   cells. Previous studies have shown that moderate autophagy can alleviate I/R injury in heart,

61   brain and renal by eliminating damaged mitochondria reducing oxidative stress and free radical

62   production (*Li et al., 2013; Ling et al., 2011; Rautou et al., 2010*), but excessive eliminating

63   mitochondria could cause cell death, namely atophagic cell death. *Amadoro et al. (2014)* have

64   demonstrated that excessive mitophagy was involved in many disease process, such as

65   neurodegenerative diseases immunological diseases, and cancers. Therefore, we speculated that

66   excessive mitophagy may be a new therapeutic target for HIRI.

67   N-acetyl-L-tryptophan (L-NAT), a potent scavenger of ROS and inhibitor of cytochrome c

68   release from mitochondria, is reported to provide neuroprotection in neurodegenerative diseases

69   (*Li et al., 2015*), such as reducing the damage of Parkinson's disease (*Thornton et al., 2012*) and

70   alleviating brain edema and axonal injury in traumatic brain injury and stroke (*Vink et al., 2004;*

71   *Donkin et al., 2009; Turner et al., 2005*). Another study also showed that L-NAT, an antagonist

72   of the neurokinin 1 receptor (NK-1R) known to disrupt the binding of Substance P (SP) to NK-

73   1R, played a protective role on neurodegenerative diseases (*Sirianni et al., 2015*). Our previous

74   studies indicated that L-NAT could not only reduce the damage of the primary hippocampal

75   neurons and NSC-34 cells induced by hydrogen peroxide (H_2O_2) in vitro, but also alleviate ALS

76   and cerebral ischemia / hypoxia injury in mouse model in vivo (*Codogno et al., 2013; Jiang et*

77   *al., 2014*). Our recent work confirmed that L-NAT has hepatoprotective effects in vitro and vivo

78 through inhibiting the disruption of hepatocytes,improving the cell viability, attenuating the

79 inflammation and the expression of RIP2, Caspase-1 and IL-1β (*Wang et al., 2019*). However,

80 the relationship between mitophagy and the hepatoprotective of L-NAT are not fully understood.

81 In this study, we investigated the effects of L-NAT on hepatocytes morphology, the structure and

82 function of mitochondria, and activation of autophagy during the period of HIRI, which may

83 provide experimental evidence for application of L-NAT on HIRI.

Materials and Methods

Chemicals

86 L-NAT, Beclin1, microtubule- associated protein 1 light chain 3-Ⅱ (LC3-Ⅱ), autophagy

87 related protein 7 (ATG-7), SQSTM1 (P62) antibodies and 3-Methyladenine (3-MA) were

88 purchased from Sigma-Aldrich (St.Louis, MO, USA) and GAPDH antibody was obtained from

89 Proteintech Group (Chicago, USA). Secondary anti-rabbit antibody was purchased from

90 Amersham Pharmacia Biotech (Piscataway, NJ). The enhanced chemiluminescence (ECL)

91 system was obtained from Amersham Pharmacia Biotech (Piscataway, NJ). RIPA lysis was

92 purchased from Solarbio (Beijing, China). The cell counting kit-8 (CCK-8) was purchased from

93 7sea-Biotech (Shanghai, China). ATP assay kit was purchased from Beyotime Biotechnology

94 (Shanghai, China) and MitoTracker Red kit came from Yeasen Biotech (Shanghai, China) and

95 DAPI came from Life Technologies.

Animals

97 Healthy male Sprague-Dawley (SD) rats weighing 200-220 g were purchased from Pengyue

98 experimental animal center in Jinan, China (Shandong Experimental Animal Center provided full

99 approval for this research (No.37009200010769)). They were randomly divided into sham group,

100 I/R group, and I/R + L-NAT group, with 6 rats in each group. Rats were fasted for 12 h before

101 surgery, and were given free access to water. In I/R + L-NAT group, L-NAT (10 mg / kg) was

102 intraperitoneal injected 30 min before modeling (*Wang et al., 2019*). The rats were anesthetized

103 by intraperitoneal injection of ketamine, the left and middle branches of the hepatic pedicle were

104   occluded with a non-traumatic vascular clamp in I/R + L-NAT group and I/R group. The success

105   of the model was apparent once the liver color turned from red to dark purple. After 45 min of

106   ischemia, the clip was removed to allow hepatic reperfusion. In sham group, the rats underwent

107   the same surgery but no vessel clamps were placed. According to the previous literature of our

108   laboratory, the most obvious liver function damage was after 6 h of reperfusion, so we took the

109   liver tissue after 6 h of reperfusion. The Animal Ethics Committee of the University approved all

110   working protocols.

Cell culture and treatment

112   The rat hepatocyte BRL cell line was purchased from the Chinese Academy of Sciences

113   Cell Bank (Shanghai, China). BRL cells were cultured in a 37 °C incubator which is a

114   humidified environment of 95% air/5% CO_2. The cells were divided into three groups: control

115   group, H_2O_2 group and H_2O_2 + L-NAT group. Referring to the previous literature in our

116   laboratory, oxidative damage model of BRL cells were prepared by pre-treatment with 200 μM

117   H_2O_2 for 6 h. And H_2O_2 + L-NAT group was pre-treated with 10 μM L-NAT for 2 h before

118   adding H_2O_2 (*Wang et al., 2019*).

Cell Viability Assay

120   Cell viability was determined using CCK-8 colorimetric kit. BRL cells were adjusted as

121   2×10^5 cells / mL, then were inoculated in 96-well plate with 100 μL / well and were cultured

122   overnight, when a partial monolayer was formed. Then, cells were exposed to 200 μM H_2O_2 with

123   or without L-NAT for 6 hours. Subsequently, cells were cultured in a solution of 100 μL CCK-8

124   / mL DMEM for 1 h in a CO_2 incubator in darkness. The absorbance of the sample was

125   measured at 450 nm using a microplate reader (Thermo, Massachusetts, USA). The experiments

126   were performed in 5 replicate holes and repeated three times.

Enhanced ATP assay

128   The level of intracellular ATP was determined according to the instructions using an ATP

129   assay kit. A same amount of BRL cells in 6-well plates were lysed and centrifuged at 12000 g for

130   5 min at 4 °C. Subsequently, 20 μL of the supernatant was mixed with 100 μL of luciferase

131   reagent in an opaque 96-well plate and was measured using the chemiluminometer.

132 **Transmission election microscopy (TEM)**

133   The perfused liver tissue was fixed in PBS (pH = 7.4) containing 2.5% glutaraldehyde for at

134   least 2 h, which was then fixed in 1% osmium tetroxide for 1 h at 4 °C temperature. Tissues were

135   embedded in an epoxy resin and made into 100 nm ultrathin slices. The ultrastructure of the

136   sample was observed using TEM (JEM. 1010, JEOL, Tokyo, Japan).

137 **Immunofluorescence technique**

138   Liver tissue was perfused and fixed, and 10-μm-thick frozen sections were prepared, fixed

139   in 4% paraformaldehyde for 15 min, and washed with PBS. The endogenous peroxidase was

140   inactivated by blocking with 1% goat serum for 30 min at room temperature and then incubated

141   overnight at 4 °C with diluted primary antibody (LC3-II, 1:200, Sigma; Beclin1, 1:200, Sigma;

142   ATG-7, 1:200, Sigma; P62, 1:200, Sigma). The following day, it was washed three times with

143   PBS, incubated with the secondary antibody for 60 min at room temperature, washed three times

144   with PBS, and nucleus were stained by DAPI (1 mg / mL), then observed under the fluorescence

145   microscope (Olympus, Japan).

146 **MitoTracker staining mitochondria**

147   After seeding cells on coverslips and treating with the drug, according to the instructions of

148   MitoTracker Red CMXRos kit (Yeasen, Shanghai, China), 200 nM H-DMEM medium was

149   added onto each slide, and then incubated in 37 °C incubator for 30 min. Cells were washed with

150   PBS, and fixed with paraformaldehyde and permeabilized with cold acetone, then observed cells

151   under the fluorescence microscope (Olympus, Japan).

152 **Rhodamine 123 Staining**

153   BRL cells were cultured on slide and pretreated with 10 μM L-NAT for 2 h and then treated

154   with 200 μM H_2O_2 for 6 h. Mitochondrial membrane potential was determined using rhodamine

155   123, a kind of lipophilic cationic fluorescent dye that can pass through the cell membrane of live

156 cells for detecting mitochondrial membrane potential (*Jiang et al., 2014*). Briefly, the processed

157 cells were directly incubated with 2 μM rhodamine 123 for 40 min in 37 °C CO_2 incubator in

158 dark, followed by rinsing with PBS, and stained nucleus with DAPI (1 mg / mL). Images were

159 taken using a fluorescence microscope.

Flow Cytometry

161   BRL cells were adjusted to 2×10^5 cells / mL, then were inoculated in 6-well plate with 1

162 mL / well and cultured overnight. After treatment with L-NAT and H_2O_2, then cells were

163 collected into centrifuge tubes and centrifuged at 2000 rpm for 5 min, the supernatant was

164 discarded and PBS was added. Rhodamine 123 was added to the suspension at a concentration of

165 2 μg / mL, incubated at 37 ° C for 40 min, and then centrifuged at 2000 rpm for 5 min. Cells

166 were washed twice with PBS, and detected by flow cytometry. The excitation wavelength was

167 507 nm, and the emission wavelength was 530 nm.

Quantitative Real-time PCR *(qRT-PCR)*

169   Total RNA was extracted from the treated liver tissue and BRL cells according to the

170 instructions of TRIzol agentia (Life, USA), to reverse transcripted in cDNA and PCR

171 amplification was performed with 20 μL reaction system (*Wang et al., 2019*). The primers used

172 in this study were as follows:

Western Blotting

174   Tissue or cells were exposed to the mixture of RIPA lysis buffer and phenylmethylsulfonyl

175 (PMSF) fluoride, lysed on ice, and centrifuged at 12000 g for 15 min at 4 °C to extract total

176 protein and protein concentration was determined by BCA method. Proteins were separated by

177 electrophoresis and then transferred onto a PVDF membrane by electro-blotting. Samples were

178 incubated overnight at 4 °C with antibodies such as LC3-II (1:500), Beclin1 (1:500), ATG-7

179 (1:200), P62 (1:500) and GAPDH (1:1000). The images were analyzed by ImageJ software. The

180 results were normalized to the ratio of target protein optical density values to those of the internal

181 reference protein GAPDH.

Statistical analysis

All experiments were repeated three times and data were presented as the mean ± SD values. Statistical analyses of the data were performed using a one-way analysis of variance (ANOVA) followed by the least significant difference (LSD) test with Statistical Package for the Social Sciences (SPSS, version 22.0) software, $p < 0.05$ were considered statistically significant.

Results

2.1 Effect of L-NAT on autophagy after hepatic ischemia-reperfusion injury

Given the evidence that excessive autophagy related to hepatocyte injury during HIRI, and the modulation of autophagy may render hepatocyte resistant to I/R injury. Subsequently, the change of autophagy activation was investigated. The times sequential changes of Beclin1 was investigated by qRT-PCR and Western Blotting during 0 h, 1 h, 4 h, 6 h, 12 h and 24 h of reperfusion, as shown in Figs. 1A-1C, both the mRNA and protein expression of Beclin1 peaked at 6 h after reperfusion. Accordingly, rats were subjected to 45 min of hepatic ischemia followed by reperfusion 6 h for subsequent experiments.

To understand whether L-NAT could reduce autophagy activation, we next investigated the expression of autophagy markers (LC3-Ⅱ, Beclin1, ATG-7 and P62) after HIRI present with or without L-NAT using the Rat HIRI model and H_2O_2-induced oxidative damage. Results of qRT-PCR and Western Blotting showed that the expression levels of LC3-II, Beclin1, and ATG-7 in I/R group showed an increase than those in sham group, while the P62 level dropped to 0.6-fold, and L-NAT administration could reverse those changes of autophagy markers (Figs. 2A-2I). Immunofluorescence assays showed that LC3-II, Beclin1, and ATG-7 staining (green fluorescence) increased, P62 staining (green fluorescence) significantly decreased in I/R group compared with the sham group (Fig. 2J). As shown in Figs. 3A-3J, results in vitro are consistent with that in vivo. These data indicated that L-NAT could regulate the expression of autophagic protein during HIRI injury.

To confirm the protective effect of L-NAT on HIRI-induced autophagy, the autophagosome

208   in hepatocyte were observed by EM. Results showed that most of autophagosomes in I/R group,

209   showed monolayer membrane, wrapped the degraded mitochondria and other cytosolic

210   component. Meanwhile, in I/R group, autophagosome volume is increased approximately 1.5–2

211   times larger than that in sham group. And all those morphological changes of autophagosomes

212   were reversed by L-NAT pretreated (Figs. 4). Those data demonstrated that L-NAT could

213   decrease the formation of autophagosome.

214   2.2 Effects of L-NAT on mitochondrial structure

215   A large body of evidence indicates that mitochondrial dysfunction plays a key role in I/R

216   injury in heart, brain, liver, kidney and other organs. To investigate whether the effect of L-NAT

217   on I/R is related to mitochondrial protection, we investigated the effect of L-NAT on

218   mitochondrial morphology. EM analysis showed that mitochondria of hepatocyte in sham group

219   were evenly distributed in the cytoplasm, with well-arranged cristae structure, while the number

220   of mitochondria in I/R group increased and was centralized distribution around the nucleus, the

221   mitochondrial cristaes were disordered, while the damaged mitochondria were phagocytosed by

222   the vacuolar structure. L-NAT pretreatment improved morphological changes of mitochondria

223   induced by I/R injury (Figs. 5).

224   2.3 Effects of L-NAT on mitochondrial function

225   ATP, produced by mitochondria, is the main form of intracellular energy supply. To

226   investigate whether L-NAT improves mitochondrial function changes caused by HIRI, we

227   measured the ATP content in H_2O_2-induced oxidative damage model with or without L-NAT.

228   Results showed that compared with control group, H_2O_2-mediated BRL cells caused

229   mitochondrial damage, resulting in a ATP decrease of 0.35-fold, which was reversed to 0.8-fold

230   by L-NAT pretreatment. Those changes of ATP indicated that L-NAT can rescue mitochondrial

231   function (Fig. 6 A).

232   The above results showed that L-NAT can protect mitochondrial structure and ATP which

233   is caused by I/R-induced, thereby alleviating mitochondrial dysfunction. A large body of

234   evidence indicated that thirteen kinds of proteins encoded by mitochondrial DNA (mtDNA) are

235   closely related to mitochondrial function, and maintaining stability of the quantity and quality of

236   mtDNA are critical for the maintenance of mitochondrial function. In order to clarify the effect

237   of L-NAT on mtDNA changes after I/R, we designed primers for the coding genes ND1 and

238   COX-1 of mtDNA heavy and light chains to detect copy number of mtDNA. Additionally

239   mtAtp6 is used to represent mtDNA (*Codogno et al., 2013*), and expression of Rp113 is used to

240   represent cellular total DNA, therefore, the ratio of them represents the content of mitochondria

241   in each cell. Subsequently, qRT-PCR was used to detect the expression of the ND1, COX-1,

242   mtAtp6 and Rp113 in I/R-mediated oxidative stress injury model. We found that the radio of

243   mtAtp6 / Rp113 was increased, which is 1.42-fold higher than that in sham group, and the

244   expression of ND1 and COX-1 was attenuated to 0.67-fold and 0.74-fold in I/R group compared

245   with sham group, respectively. The L-NAT pre-treatment group significantly improved these

246   changes (Figs. 6B-6D). Taken together, the experimental results provided strong evidence that

247   maintaining the quantity and quality of mtDNA stability might be closely related to the

248   protective effect of L-NAT.

249   As an extension of the above results, the mitochondrial transmembrane potential ($\Delta\Psi_m$)

250   assay was used as a specific test for the earliest events of mitochondrial injury. The results

251   showed that rhodamine 123 fluorescence in control group cells showed a punctate distribution,

252   which has an appearance of a grainy rhodamine 123 fluorescence in cytoplasm. Upon H_2O_2

253   exposure, the fluorescent signal from rhodamine 123 becomes diffuses, which was considered a

254   diffused pattern. L-NAT pretreatment reversed the H_2O_2-induced dissipation of rhodamine123

255   fluorescence, indicating that $\Delta\Psi_m$ was maintained (Figs. 6E-6F).

256   In addition to the rhodamine 123 staining pattern, the fluorescence intensity was also

257   investigated. As shown in Fig. 6G, the fluorescence intensity of rhodamine 123 in H_2O_2 group

258   decreased significantly compared to the untreated group, which implied the loss of $\Delta\Psi_{m,}$ and L-

259   NAT administration significantly inhibited the decreased fluorescence intensity induced by H_2O_2.

260   Those data provide evidence that L-NAT pretreatment could prevent the dissipation of $\Delta\Psi_m$

261   induced by H_2O_2.

2.4 Effect of L-NAT on mitophagy

262

263 To further explore whether the protective effect of L-NAT on hepatocytes was achieved by

264 acting on mitophagy, we first measured the level of Beclin1 in H_2O_2-mediate BRL cells by

265 immunofluorescence staining, then labeled mitochondrial by MitoTracker to observe the changes

266 of mitophagy in H_2O_2-mediated BRL oxidative damage model. The data indicated that the

267 number of co-localization of Beclin1 and MitoTracker were significantly increased after H_2O_2

268 induction. L-NAT effectively reduces H_2O_2-induced the number of Beclin1 and MitoTracker

269 double positive cells induced by H_2O_2 (Fig. 7). This observation suggested that L-NAT could

270 decreased the co-location of autophagy protein and mitochondrial.

2.5 The autophagy inhibitor on cytoprotecyive effect of L-NAT

271

272 The above experiments have clarified that L-NAT can alleviate HIRI by inhibiting

273 mitophagy. Subsequently, we investigated the effect of 3-MA, an autophagy inhibitor, on the

274 hepatoprotective of L-NAT. According to preliminary experiment, the cell viability reached the

275 highest point after 5 mM 3-MA pretreatment, and 5 mM 3-MA was subjected for subsequent

276 experiments. As showed in Fig. 8A, L-NAT administration could elevate the decline of cell

277 viability which was induced by H_2O_2 and 3-MA pretreatment could reverse part of those changes.

278 Interestingly, the results of Western Blotting and qRT-PCR revealed that the combination of 3-

279 MA elevated the Beclin1 level of H_2O_2-induced BRL cells, compared with the usage of L-NAT

280 solely (Figs. 8B-8D),   implied that the autophagy inhibitor 3-MA partially weaken the

281 protective effect of L-NAT on HIRI. Taken together, these results futher identified that the

282 hepatoprotective effect of L-NAT depended on mitophagy process.

Discussion

283

284 Although the mechanism of HIRI has not been clarified, increasing evidence shows that

285 oxidative stress caused by overproduction of ROS and depletion of endogenous antioxidants play

286 a major role in contributing to tissue injury and thus liver dysfunction after HIRI. L-NAT, an

287 antagonist of NK-1R, has the effect of scavenging ROS. In the present study, we demonstrated

288   the following findings: first, we found that the changes of morphology and cell viability were

289   improved by L-NAT. Second, L-NAT could significantly decrease autophagy after HIRI and

290   resue the damage of mitochondrial structure and function. Finally, the hepatoprotecive effect of

291   L-NAT was reversed by autophagy inhibitor. These findings implied that the protective effect of

292   L-NAT on hepatocytes was closely related to inhibiting the excessive mitophagy indunced by

293   HIRI.

294   Autophagy is a highly conservative intracellular process involving the degrading the

295   impaired proteins or damaged organelles to maintain cellular homeostasis and supply substrates

296   for energy generation, implying modulate autophagy could improve the ability of cells to

297   stimulation. Therefore, autophagy is recognized as a critical pathway in the regulation of cell

298   death and survival (*Baehrecke et al., 2005; Hou et al., 2019*). Although autophagy has been

299   investigated more and more extensively in the field of liver diseases, the exact function of

300   autophagy, which can be destructive or protective in HIRI remains controversial.

301   Studies demonstrate that autophagy plays important roles in protecting against HIRI. *Zhao*

302   *et al. (2015)* reported that ulinastatin led to an increase in Beclin1, LC3-II and a decrease in P62.

303   And 3-MA, an inhibitor of autophagy, could reverse the changes of the autophagy related

304   proteins, and made morphological damage and cell apoptosis worsen in ulinastatin-treated H / R

305   liver cells. *Lee et al. (2016)* showed that everolimus protected the liver against hepatic IRI by

306   way of activating autophagy and the blockage of autophagy, which was abrogated by either

307   bafilomycin A1 or si-autophagy-related protein 5. *Rao et al. (2018)*'s study indicated that

308   isoflurane could reduce liver injury and restore liver autophagy by elevated LC3-II protein levels

309   accompanied with increased P62 degradation. In addition, 3-MA pretreatment showed no

310   significant influence in the control group, but abrogated the protective role of isoflurane

311   preconditioning both in stressed livers. Furthermore, the beneficial effects of autophagy during

312   I/R have been reported by other researchers (*Wu et al., 2018*). The aforementioned studies

313   suggested that an upregulation of autophagy during I/R injury is protective. In the present study,

314   we demonstrated that L-NAT pretreatment decreased the expression of LC3-Ⅱ, Beclin1 and

315   ATG-7 induced by HIRI, and increased the expression of P62, which were partly abolished by

316   the combination of 3-MA. Those results implied that L-NAT likely protected hepatocyte by

317   inibiting excessive autophagy production.

318   As the center of energy production, programmed cell death, reactive oxidative

319   phosphorylation and calcium homeostasis, mitochondria plays an important role in regulating

320   cell death and mitochondrial dysfunction is the key mechanism of various diseases including IR

321   injury. As one type of selective autophagy, the major function of mitophagy is to identify and

322   eliminate damaged or dysfunctional mitochondria. It is generally perceived that the function of

323   autophagy is mainly prosurvival during I/R injury of various organs. Nevertheless, the true roles

324   of activated mitophagy in I/R injury, such as myocardial I/R Injury (*Yang et al., 2019*),

325   cerebral I/R (*Li et al., 2018*), and renal I/R (*Li et al., 2018*) etc., is still controversial. Mitophagy

326   was reported to promote the clearance of injured mitochondria and then attenuate cell death

327   induced by HIRI. *Ning et al. (2018)* demonstrated that parkin mediated mitochondrial autophagy

328   was upregulated post-HIRI, leading to decreased hepatocyte death. However, parkin deficiency

329   elevates HIRI by decreasing mitochondrial autophagy and increasing apoptosis. *Bhogal et al.*

330   *(2018)* found that autophagy within LEC is reduced accompanying IRI increased cell death. *Li et*

331   *al. (2018)* demonstrated that impairing mitophagy contributed to aggravation of hepatic

332   ischemia-reperfusion injury in aging mice. Those data directly support the idea about the

333   protective response of mitophagy against I/R injury.

334   However, excessive mitophagy and unnecessary mitochondrial clearance may sharply

335   reduce the number of mitochondria and energy production, leading to cell death and strategies

336   for suppressing mitophagy may protect cells from I/R injury (*Lan et al., 2018*). *Li et al. (2018)*

337   demonstrated that aging aggravates hepatic ischemia-reperfusion injury in mice by impairing

338   mitophagy. The degree of HIRI was aggravated by the enhancement of mitophagy and alleviated

339   by parkin silencing impaired mitophagy. *Sun et al. (2019)* found that miR-330-3p could alleviate

340   HIRI by inhibition PGAM5-induced mitophagy. In this study, we found that L-NAT not only

341   resue the damage of mitochondrial structurecan, but also ameliorate the damage of ATP, mtDNA

342   and loss of $\Delta\Psi m$ which induced by HIRI. Co-localization of the mitochondrial marker,

343   MitoTracker, and Beclin1, the autophagosomal marker, was reduced by L-NAT undering H_2O_2-

344   induced. Furthermore, the experiment in vitro also showed that autophagy inhibitor 3-MA

345   intervening led to an increase of beclin1 expression in BRL cells exposed to H_2O_2 treatment.

346   These findings further supported that the hepatoprotecive of L-NAT is achieved by inhibiting

347   excessive mitophagy.

348   Taken together, these results suggested that hepatic ischemia and 6 h after reperfusion

349   trigger excessive mitophagy, and L-NAT ameliorates I/R-induced hepatic injury through

350   regulation of excessive mitophagy.

351   **Conclusion**

352   The present findings demonstrated that excessive mitophagy involved in the process of

353   HIRI and L-NAT may protect hepatocytes against HIRI by inhibiting activation of excessive

354   mitophagy and improving the structure and function of mitochondria.

355   **ADDITIONAL INFORMATION AND DECLARATIONS**

356   **Acknowledgments**

357   We are grateful to Zhijun Liu who is an assistant professor and has worked in the University

358   of Massachusetts Medical School for 8 years, to correct English grammar, spelling and sentence

359   structure throughout the manuscript.

360   **Author Contributions**

361   ● Jiying Jiang and Jianguo Li designed the experiments, interpreted the results, and critically

362   revised the manuscript.

363   ● Huiting Li and Yitong Pan performed the experiments and wrote the manuscript.

364   ● Hongjuan Wu performed the morphological experiment.

365   ● Jianxin Wang and Jie Zheng analyzed the data and generated figures.

366   ● Shuna Yu and Can Wang performed the interpretation of data for the work and revised the

367   manuscript.

368   **Data Availability**

369   The following information was supplied regarding data availability:

370   The raw measurements are available in the Supplemental Files.

371 **REFERENCES**

372 Amadoro G, Corsetti V, Florenzano F, Atlante A, Ciotti MT, Mongiardi MP, Bussani R, Nicolin V, Nori

373   SL, Campanella M, Calissano P. 2014. AD-linked, toxic NH2 human tau affects the quality control of

374   mitochondria in neurons. *Neurobiol Dis* 62:489-507 DOI: 10.1016/j.nbd.2013.10.018

375 Baehrecke E. 2005. Autophagy: dual roles in life and death? *Nat Rev Mol Cell Biol* 6(6):505-10 DOI:

376   10.1038/nrm1666.

377 Bhogal RH, Weston CJ, Velduis S, G D Leuvenink H, Reynolds GM, Davies S, Nyguet-Thin L, Alfaifi M, Shepard

378   EL, Boteon Y, Wallace L, Oo YH, Adams DH, Mirza DF, Mergental H, Muirhead G, Stephenson BTF,

379   Afford SC. 2018. The Reactive Oxygen Species-Mitophagy Signaling Pathway Regulates Liver Endothelial

380   Cell Survival During Ischemia/Reperfusion Injury. *Liver Transpl* 24(10):1437-1452 DOI:10.1002/lt.25313

381 Chin R, Panavas T, Brown J, Johnson K. 2018. Patient-derived lymphoblastoid cell lines harboring mitochondrial

382   DNA mutations as tool for small molecule drug discovery. *BMC Res Notes* 11(1) :205 DOI:

383   10.1186/s13104-018-3297-6

384 Codogno P, Meijer A. 2013. Autophagy in the liver. *J Hepatol* 59(2):389-391 DOI: 10.1016/j.jhep.2013.02.031

385 Cursio R, Colosetti P, Gugenheim J. 2015. Autophagy and liver ischemia-reperfusion injury. *Biomed Res Int*

386   2015:417590 DOI: 10.1155/2015/417590

387 Donkin J, Nimmo A, Cernak I, BlumbergsP, Vink R. 2009. Substance P is associated with the development of brain

388   edema and functional defificits after traumatic brain injury. *J Cereb Blood Flow Metab* 29:1388–1398

389 Hou, J, Rao M, Zheng W, Fan J, Law B. 2019. Advances on Cell Autophagy and Its Potential Regulatory Factors in

390   Renal Ischemia-Reperfusion Injury. *DNA Cell Biol* DOI: 10.1089/dna.2019.4767

391 Jiang J,Yu S, Jiang Z, Liang C, Yu W, Li J, Du X, Wang H, Gao X, Wang X. 2014. N-acetyl-serotonin protects

392   HepG2 cells from oxidative stress injury induced by hydrogen peroxide Oxid Med Cell Longev. 2014:

393   310504 DOI: 10.1155/2014/310504

394 Ji J, Kline A, Amoscato A, Samhan-Arias A, Sparvero L, Tyurin V, Tyurina Y, Fink B, Manole M, Puccio A,

395   Okonkwo D, Cheng J, Alexander H, Clark R, Kochanek P, Wipf P, Kagan V, Bayir H. 2012. Lipidomics

396   identifies cardiolipin oxidation as a mitochondrial target for redox therapy of brain injury. *Nature*

397   *Neuroscience* 15(10):1407-1413 DOI: 10.1038/nn.3195

398   Kalimeris K, Briassoulis P, Ntzouvani A, Nomikos T, Papaparaskeva K, Politi A, Batistaki C, Kostopanagiotou

399   G.2016. N-acetylcysteine ameliorates liver injury in a rat model of intestinal ischemia reperfusion. *Journal of*

400   *Surgical Research* 206(2):263-272 DOI: 10.1016/j.jss.2016.08.049

401   Lan R, Zhang Y, Wu T, Ma YZ, Wang BQ, Zheng HZ, Li YN, Wang Y, Gu CQ, Wu JT. 2018. Xiao-Xu-Ming

402   Decoction   Reduced Mitophagy Activation   and   Improved Mitochondrial Function   in

403   Cerebral Ischemia and Reperfusion Injury. B*ehav Neurol* DOI: 10.1155/2018/4147502

404   Lee SC, Kim KH, Kim OH, Lee SK, Kim SJ. 2016. Activation of autophagy by everolimus confers hepatoprotection

405   against ischemia-reperfusion injury. *Am J Transplant* 16(7):2042-54 DOI: 10.1111/ajt.13729

406   Li F, Tan J, Zhou F, Hu Z, Yang B. 2018. Heat Shock Protein B8 (HSPB8) Reduces Oxygen-Glucose

407   Deprivation/Reperfusion Injury via the Induction of Mitophagy. *Cellular Physiology and Biochemistry* 48

408   (4):1492-1504 DOI: 10.1159/000492259

409   Li L, Chen Y, Gibson S. 2013. Starvation-induced autophagy is regulated by mitochondrial reactive oxygen species

410   leading to AMPK activation. *Cellular Signalling* 25(1): 50-65 DOI: 10.1111/jpi.12337

411   Lin C, Chao H, Li Z, Xu X, Liu Y, Hou L, Liu N, Ji J. 2016. Melatonin attenuates traumatic brain injury-induced

412   inflammation: a possible role for mitophagy. *J Pineal Res* 61(2): 177-186

413   Ling L, Tan K, Lin H, Chiu G. 2011. The role of reactive oxygen species and autophagy in safingol-induced cell

414   death. *Cell Death & Disease* 2:129 DOI: 10.1038/cddis.2011.12

415   Li N, Wang H, Jiang C, Zhang M. 2018. Renal ischemia/reperfusion-induced mitophagy protects against renal

416   dysfunction via Drp1-dependent-pathway. *Exp Cell Res* 369 (1):27-33 DOI: 10.1016/j.yexcr.2018.04.025

417   Li W, Fotinos A, Wu Q, Chen Y, Zhu Y, Baranov S, Tu Y, Zhou E, Sinha B, Kristal B, Wang X. 2015. N-acetyl-L-

418   tryptophan delays disease onset and extends survival in an amyotrophic lateral sclerosis transgenic mouse

419   model. *Neurobiol Dis* 80:93-103 DOI: 10.1016/j.nbd.2015.05.002

420   Li Q, Gao S, Kang Z, Zhang M, Zhao X, Zhai Y, Huang J, Yang G, Sun W, Wang J. 2018. Rapamycin Enhances

421   Mitophagy and Attenuates Apoptosis After Spinal Ischemia-Reperfusion Injury. *Front Neurosci* 12:865

422   DOI: 10.3389/fnins.2018.00865

423   Li Y, Ruan DY, Jia CC, Zheng J, Wang GY, Zhao H, Yang Q, Liu W, Yi SH, Li H, Wang GS, Yang Y, Chen GH,

424   Zhang Q. 2018. Aging aggravates hepatic ischemia-reperfusion injury in mice by impairing mitophagy with

425   the involvement of the EIF2α-parkin pathway. *Aging (Albany NY)*. 10(8):1902-1920 DOI:

426   10.18632/ aging.101511

427   Mizunoe Y, Kobayashi M, Sudo Y, Watanabe S, Yasukawa H, Natori D, Hoshino A, Negishi A, Okita N, Komatsu

428   M, Higami Y. 2018. Trehalose protects against oxidative stress by regulating the keap1-Nrf2 and

429   autophagy pathways. *Redox Biol.* 15:115-124 DOI: 10.1016/j.redox.2017.09.007

430   Ning XJ, Yan X, Wang YF, Wang R, Fan XL, Zhong ZB, Ye QF. 2018. Parkin deficiency elevates

431   hepatic ischemia/reperfusion injury accompanying decreased mitochondrial autophagy, increased apoptosis,

432   impaired DNA damage repair and altered cell cycle distribution. *Mol Med Rep* 18(6):5663-5668 DOI:

433   10.3892/mmr.2018.9606

434   Park S, Chen S, Kim M, D'Agati V, Lee H. 2009. Human activated protein C attenuates both hepatic and renal

435   injury caused by hepatic ischemia and reperfusion injury in mice. *Kidney International* 76(7):739-750 DOI:

436   10.1038/ki.2009.255

437   Rao Z, Pan X, Zhang H, Sun J, Li J, Lu T, Gao M, Liu S, Yu D, Ding Z. 2017. Isoflurane preconditioning alleviated

438   murine liver ischemia and reperfusion injury by restoring AMPK/mTOR-mediated autophagy. *Anesth*

439   *Analg* 125(4):1355-1363 DOI: 10.1213/ANE

440   Rautou P, Mansouri A, Lebrec D, Durand F, Valla D, Moreau R. 2010. Autophagy in liver diseases. *Journal of*

441   *Hepatology* 53(6) :1123-1134 DOI: 10.1016/j.jhep.2010.07.006

442   Selzner N, Rudiger R, Clavien P. 2003. Protective strategies against ischemic injury of the liver. *Gastroenterology*

443   125(3):917-936 DOI: 10.1016/s0016-5085(03)01048-5

444   Shadel G, Horvath T. 2015. Mitochondrial ROS signaling in organismal homeostasis. *Cell* 163(3):560-569 DOI:

445   10.1016/j.cell.2015.10.001

446   Singh A, Kukreti R, Saso L, Kukreti S. 2019. Oxidative stress: a key modulator in neurodegenerative diseases.

447   *Molecules* 22;24(8) DOI: 10.3390/molecules24081583

448   Sirianni AC, Jiang J, Zeng J, Mao LL, Zhou S, Sugarbaker P, Zhang X, Li W, Friedlander RM, Wang X. 2015. N-

449   acetyl-l-tryptophan, but not N-acetyl-d-tryptophan, rescues neuronal cell death in models of amyotrophic

450    lateral sclerosis. *J Neurochem* 134(5):956-68 DOI: 10.1111/jnc.13190

451 Sun XL, Zhang YL, Xi SM, Ma LJ, Li SP. 2019. MiR-330-3p suppresses phosphoglycerate mutase family member

452    5 -inducted mitophagy to alleviate hepatic ischemia-reperfusion injury. *J Cell Biochem* 120(3):4255-4267

453    DOI: 10.1002/jcb.27711

454 Thornton E, Vink R. 2012. Treatment with a Substance P Receptor Antagonist Is Neuroprotective in the Intrastriatal

455    6-Hydroxydopamine Model of Early Parkinson's Disease. *Plos One* 7(4) DOI: ARTN e34138

456 Turner R, Blumbergs P, Vink R. 2005. A substance P antagonist improves outcome following reversible middle

457    cerebral artery occlusion in rats. *J Cereb Blood Flow Metab* S32

458 Vink R, Donkin J, Cruz M, Nimmo A, Cernak I. 2004. A substance P antagonist increases brain intracellular free

459    magnesium concentration after diffuse traumatic brain injury in rats. *J Am Coll Nutr* 23 (5):538S-540S

460 Wang B, Su CJ, Liu TT, Zhou Y, Feng Y, Huang Y, Liu X, Wang ZH, Chen LH, Luo WF, Liu T. 2018. The

461    Neuroprotection of Low-Dose Morphine in Cellular and Animal Models of Parkinson's Disease Through

462    Ameliorating Endoplasmic Reticulum (ER) Stress and Activating Autophagy. *Front Mol Neurosci* 20;

463    11:120 DOI: 10.3389/fnmol.2018.00120

464 Wang J, Yu S, Li J, Li H, Jiang H, Xiao P, Pan Y, Zheng J, Yu L, Jiang J. 2019. Protective role of N-acetyl-

465    tryptophan against hepatic ischemia-reperfusion injury via the RIP2/caspase-1/IL-1βsignaling pathway.

466    *Pharmaceutical Biology* 57(1):385-391 DOI: 10.1080/13880209

467 Wu X, Li X, Liu Y, Yuan N, Li C, Kang Z, Zhang X, Xia Y, Hao Y, Tan Y. 2018. Hydrogen exerts neuroprotective

468    effects on OGD/R damaged neurons in rat hippocampal by protecting mitochondrial function via regulating

469    mitophagy mediated by PINK1/Parkin signaling pathway. *Brain Res* 1698:89-98 DOI:

470    10.1016/j.brainres.2018.06.028.

471 Yang M, Linn B, Zhang Y, Ren J. 2019. Mitophagy and mitochondrial integrity in cardiac ischemia-reperfusion

472    injury. *Biochim Biophys Acta Mol Basis Dis* 1865 (9):2293-2302 DOI: 10.1016/j.bbadis.2019.05.007

473 Zhao Y, Cai H, Zhou P, Lin S, Pan Y, Liang X. 2019. Protective effect of ulinastatin on hepatic ischemia

474    reperfusion injury through autophagy activation in Chang liver cells. *J Cell Biochem* 120(9):14960-

475    14970 DOI: 10.1002/jcb.28758.

Figure 1

The time-series expression of Beclin1 mRNA and protein during HIRI.

(A) The time-series expression of Beclin1 determined by qRT-PCR. (B-C) The time-series expression of Beclin1 determined by Western Blotting. The data are the mean ± SD (n=3), *p < 0.05, **p < 0.01, ***p < 0.001 compared with the related sham group.
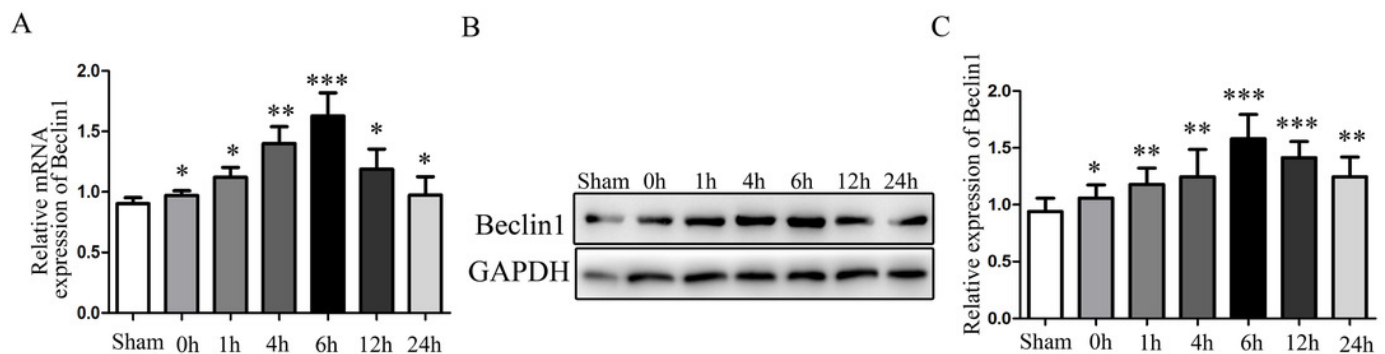
Figure 2

Changes of autophagy marker after HIRI in vivo.

(A-I) Relative mRNA and Western Blotting analysis of autophagy markers (Beclin1, LC3-II, ATG-7 and P62) in rat liver tissues (n=3). (J-U) Immunofluorescence staining (200×) in rat liver tissues, bar=50 μm. The data are the mean ± SD, *$p < 0.05$, **$p < 0.01$, ***$p < 0.001$ compared with the related sham group, #$p < 0.05$, ##$p < 0.01$, ###$p < 0.001$ compared with related I/R group.
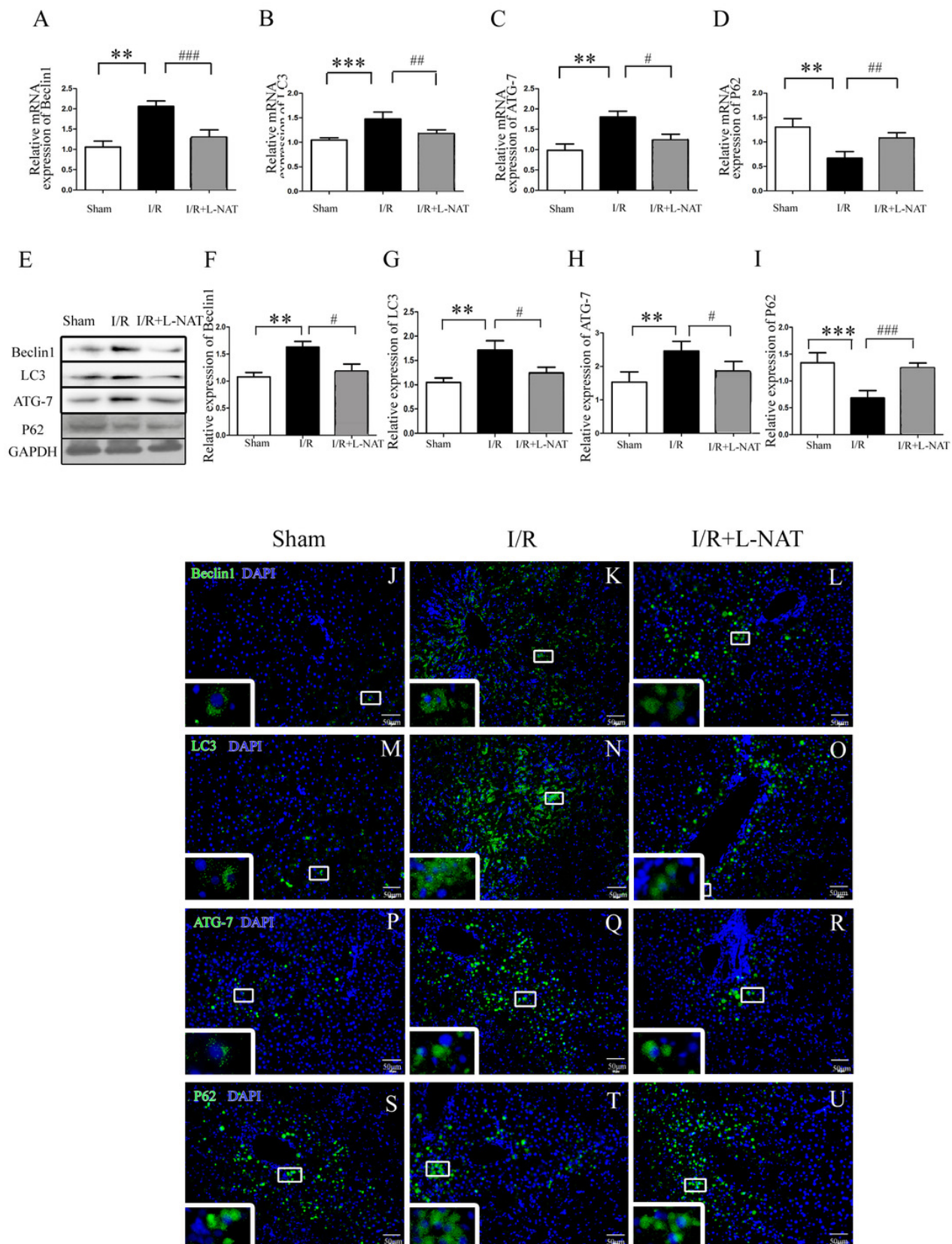
Figure 3

The changes of autophagy protein in H_2O_2-induced BRL cells in vitro.

(A-I) Relative mRNA and Western Blotting analysis of autophagy markers (Beclin1, LC3-II, ATG-7 and P62) in BRL cells (n=3). (J-U) Immunofluorescence staining (200×) in BRL cells, bar=50 μm. The data are the mean ± SD, $*p < 0.05$, $**p < 0.01$, $***p < 0.001$ compared with the related control group, $^{\#}p < 0.05$, $^{\#\#}p < 0.01$, $^{\#\#\#}p < 0.001$ compared with related H_2O_2 group.
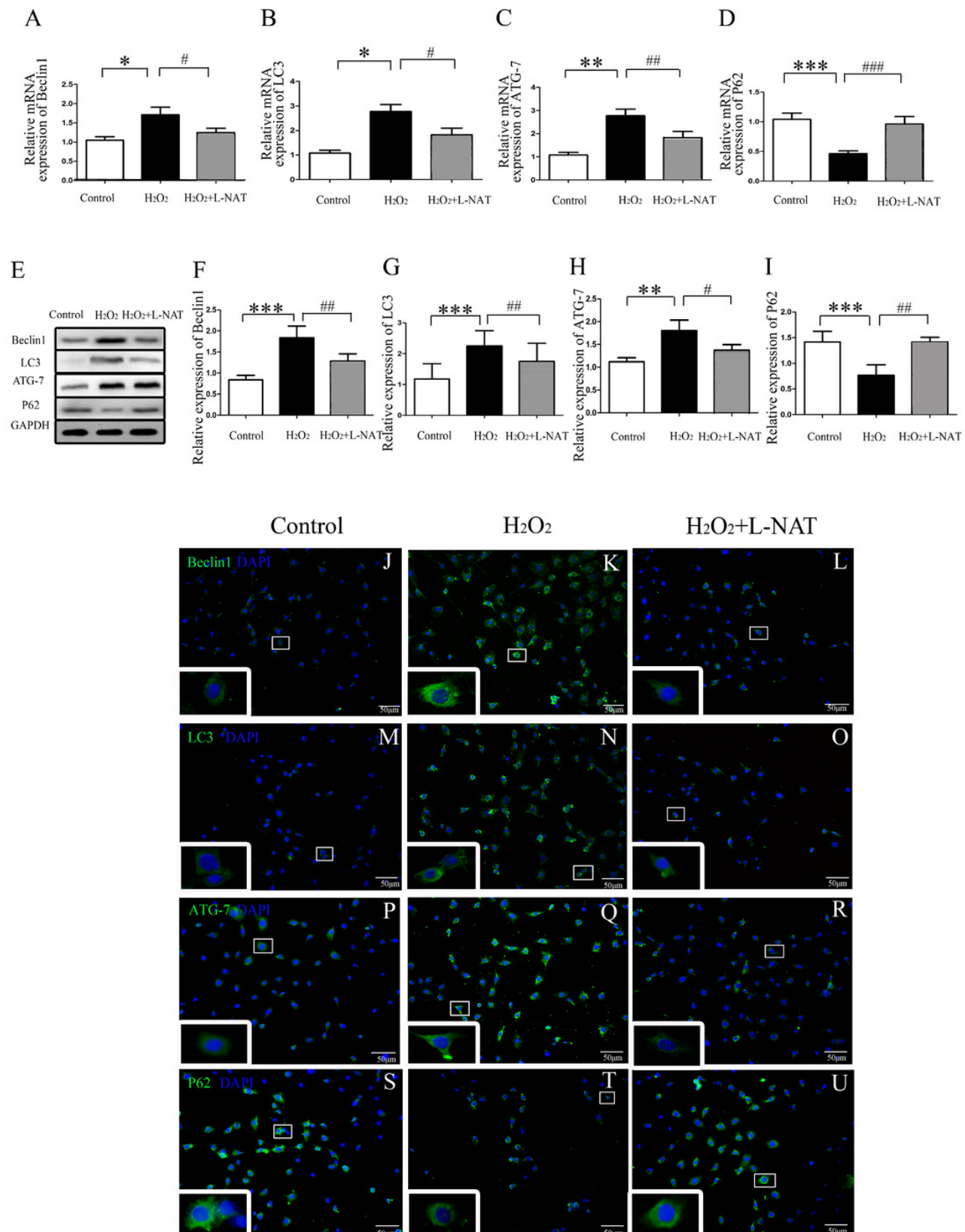
Figure 4

Changes of autophagosomes after HIRI detected by transmission electron microscopy (10000×).

(A-C) The arrows indicate autophagosomes, bar=1 μm.
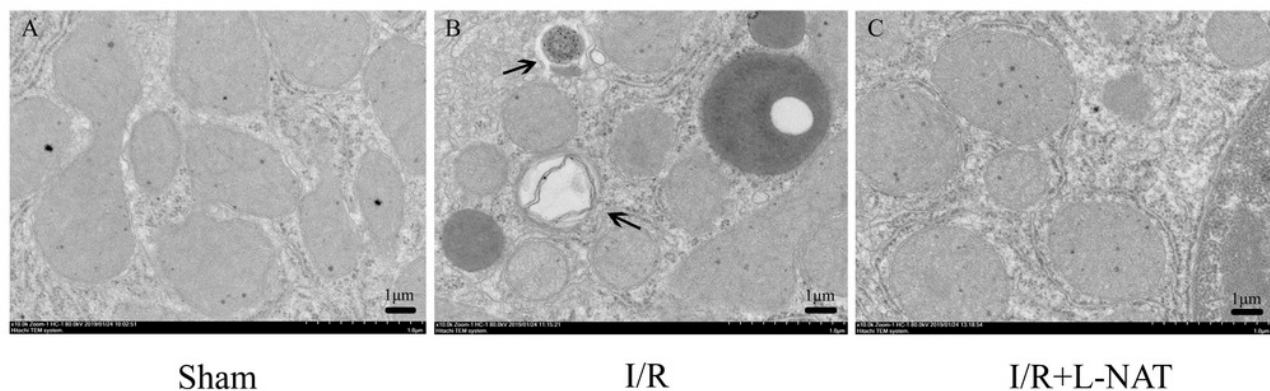
Figure 5

Changes of mitochondria after HIRI detected by transmission electron microscopy (10000×).

(A-C) The arrows indicate damaged mitochondria which were phagocytosed by the vacuolar, bar=1 μm.

| Sham | I/R | I/R+L-NAT |
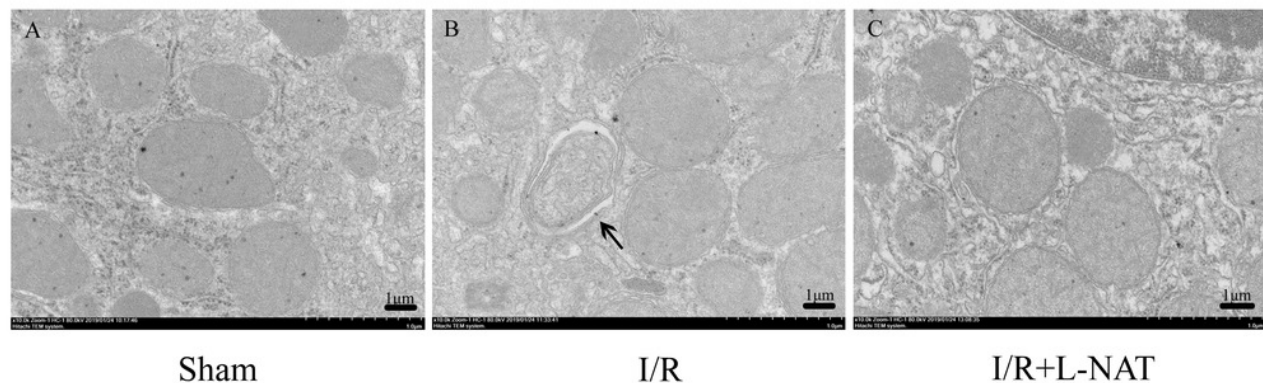
Figure 6

Effects of L-NAT on mitochondrial function after HIRI.

(A-D) ATP contention, the ratio of mtAtp6/Rp113 mRNA, the expression of ND1 mRNA and COX-1 mRNA. (E-K) Using rhodamine123 staining,mitochondrial membrane potential in BRL cells was detected by flow cytometry (E-H) and fluorescence microscope (I-K), bar=50 µm. The data are the mean ± SD, *$p < 0.05$, **$p < 0.01$, ***$p < 0.001$ compared with the related sham group, #$p < 0.05$, ##$p < 0.01$ compared with related I/R group.
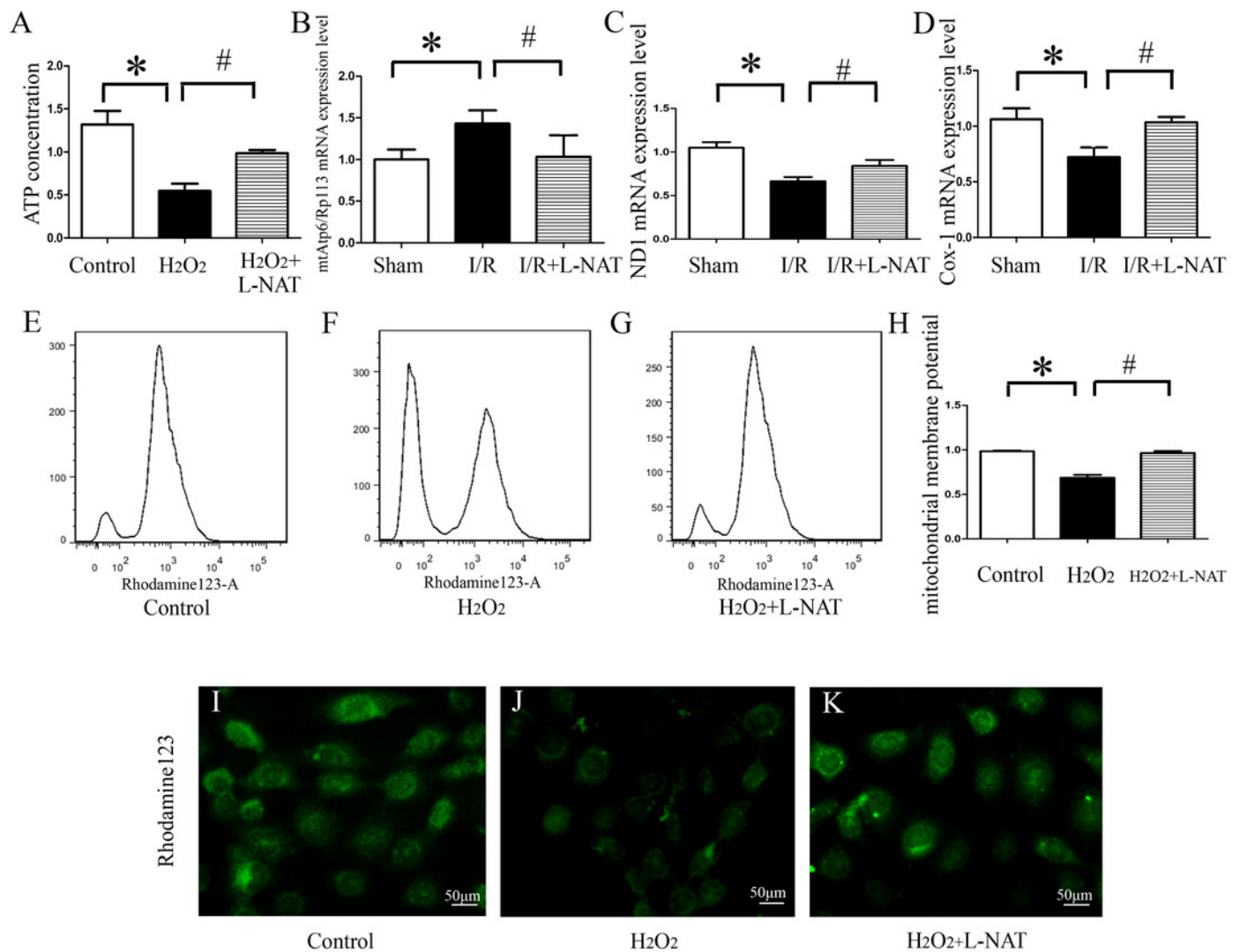
Figure 7

Colocalization of Beclin1 and MitoTracker in H_2O_2-induced BRL oxidative damage model (200×).

Bar=50 μm.
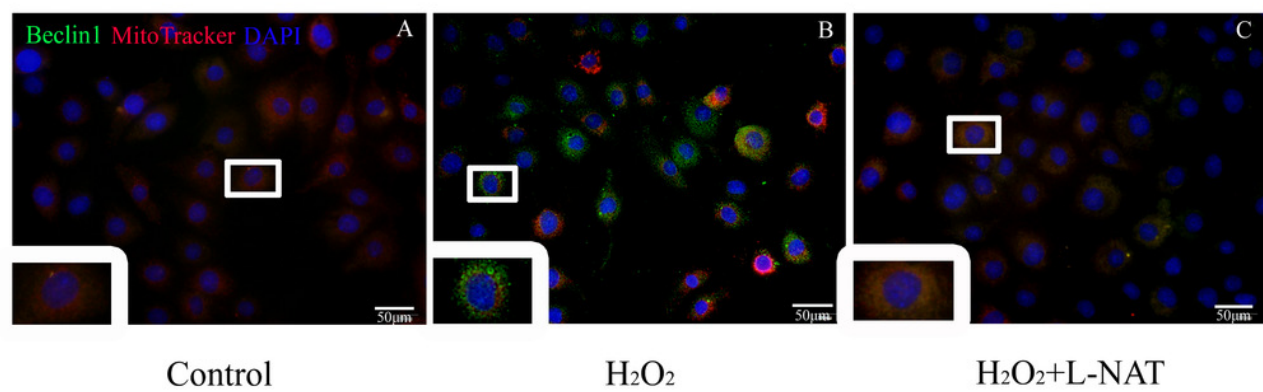
Figure 8

Effects of 3-MA on cytoprotection of L-NAT.

(A) Effects of different concentrations of autophagy inhibitors on cytoprotection of L-NAT (n=3). (B) The mRNA levels of Beclin1 in BRL cells (n=3). (C) Western Blotting analysis of Beclin1 protein expression in BRL cells (n=3). The data are the mean ± SD, *$p < 0.05$, **$p < 0.01$, ***$p < 0.001$ compared with the related group, #$p < 0.05$, ##$p < 0.01$, ##$p < 0.001$ compared with related H_2O_2 group, ▲▲$p < 0.01$ compared with related L-NAT group.